Coverage and Aggregation of Gold Nanoparticles on Silanized Glasses

Alberto F. Scarpettini*,[†] and Andrea V. Bragas[†,‡]

[†]*Departamento de Física, Facultad de Ciencias Exactas y Naturales, Universidad de Buenos Aires, 1428 Buenos Aires, Argentina, and* [‡]*IFIBA, Consejo Nacional de Investigaciones Científicas y Técnicas, Argentina*

We study the dynamics of the coverage and aggregation of gold nanoparticles over organosilanized glass substrates for different sizes of nanoparticles. We present measurements of extinction spectra and nanoparticle counting statistics and demonstrate that both methods are equivalent describing those processes. We introduce models that describe the mentioned dynamics, which are characterized by an exponential-like function with two relevant parameters: a saturation value and a characteristic time. The electrostatic repulsion plays a significant role in both processes. The aggregation is dominated by the mobility of the isolated nanoparticles, which first join in dimers and, further in time, in clusters of higher number of nanoparticles.

1. Introduction

Plasmon excitation in metal nanoparticles (NPs) and nanoparticle (NP) clusters is intensively studied due to the multiple applications these phenomena have in the nanoworld today. Ranging from chemical and biological nanosensors[1−4] to plasmonic devices[5−7] and from high spatial resolution probes for microscopy[8−10] to SERS substrates,[11−13] all the applications rely, from one side, on the ability to resonantly excite the structure and, on the other side, to manage the architecture to build the desired morphology. On the road to build plasmonic samples by using metal NPs, one wants to control the degree of coverage and aggregation, since plasmonic and, consequently, optical properties depend strongly on the number of NPs and their interaction.[14] In particular, NP-decorated silica microspheres, used as plasmonic probes,[10] base their performance for nanometer-scale imaging on the formation of small clusters which provide wavelength tunable and high field enhancement. Within this scenario is undoubtedly important to understand, characterize, and control the processes underlying the assembly of NPs in glass substrates.

In this article we study carefully the process of coverage and aggregation of organosilane-modified glasses decorated with Au NPs. Many papers have been published, which cover different aspects of the kinetics,[15−19] sintering,[20,21] morphology,[22] optical properties,[15,17,22] etc., of these kinds of samples. Our approach addresses the systematic study of optical spectra and particle counting statistics, revealing different ongoing processes depending on the scale of time. One important aspect is the monitoring of the formation of dimers, trimers, and clusters of higher order for particles of different sizes as a function of time. The goal resides in performing experiments in an extended scale of time, which naturally provides a better understanding of the whole problem of covering and aggregation. We also present two models accounting for the coverage and aggregation and compare the calculations with our experimental results.

2. Experimental Section

2.1. Materials and Instrumentation. (3-Aminopropyl)-trimethoxysilane (APTMS) was bought from Sigma-Aldrich, glass microscope slides from Pearl, and colloidal gold NPs from Ted Pella, Inc. The extinction spectra were measured with a spectrophotometer (Shimadzu UV-1800). Images of adsorbed NPs on silanized glass substrates were taken by a field emission scanning electron microscope (SEM) (Zeiss Supra 40) at short integration times to avoid an excessive electrostatic charge of the samples.

2.2. Preparation of Gold Nanoparticle Samples. Glass microscope slides substrates were first cleaned with deionized water in an ultrasonic bath for 30 min. They were then immersed in HF 5% for 30 s, washed with deionized water, and dried with nitrogen. For aminosilane derivatization, glass was immersed in APTMS aqueous solution 1:100 (pH 10) in a dark environment for 1 day. They were then thoroughly rinsed with deionized water and isopropyl alcohol to remove any physisorbed APTMS. After

*Corresponding author. E-mail: ascarpet@df.uba.ar.
(1) Cao, Y. W. C.; Jin, R. C.; Mirkin, C. A. *Science* **2002**, *297*, 1536–1540.
(2) Nath, N.; Chilkoti, A. *Anal. Chem.* **2002**, *74*, 504–509.
(3) Anker, J. N.; Hall, W. P.; Lyandres, O.; Shah, N. C.; Zhao, J.; Van Duyne, R. P. *Nature Mater.* **2008**, *7*, 442–453.
(4) Kneipp, J.; Kneipp, H.; Wittig, B.; Kneipp, K. *Nanomed.-Nanotechnol.* **2010**, *6*, 214–226.
(5) Li, K. R.; Stockman, M. I.; Bergman, D. J. *Phys. Rev. Lett.* **2003**, *91*, 227402.
(6) Maier, S. A.; Kik, P. G.; Atwater, H. A.; Meltzer, S.; Harel, E.; Koel, B. E.; Requicha, A. A. G. *Nature Mater.* **2003**, *2*, 229–232.
(7) Zou, S. L.; Schatz, G. C. *Phys. Rev. B* **2006**, *74*, 125111.
(8) Kalkbrenner, T.; Ramstein, M.; Mlynek, J.; Sandoghdar, V. *J. Microsc.* **2001**, *202*, 72–76.
(9) Anger, P.; Bharadwaj, P.; Novotny, L. *Phys. Rev. Lett.* **2006**, *96*, 113002.
(10) Scarpettini, A. F.; Pellegri, N.; Bragas, A. V. *Opt. Commun.* **2009**, *282*, 1032–1035.
(11) Chumanov, G.; Sokolov, K.; Gregory, B. W.; Cotton, T. M. *J. Phys. Chem.* **1995**, *99*, 9466–9471.
(12) Freeman, R. G.; Grabar, K. C.; Allison, K. J.; Bright, R. M.; Davis, J. A.; Guthrie, A. P.; Hommer, M. B.; Jackson, M. A.; Smith, P. C.; Walter, D. G.; Natan, M. J. *Science* **1995**, *267*, 1629–1632.
(13) Tognalli, N.; Fainstein, A.; Calvo, E.; Bonazzola, C.; Pietrasanta, L.; Campoy-Quiles, M.; Etchegoin, P. *J. Chem. Phys.* **2005**, *123*, 044707.
(14) Kreibig, U.; Vollmer, M. *Optical Properties of Metal Clusters*; Springer-Verlag: Berlin, 1995; pp 124−202.

(15) Grabar, K. C.; Smith, P. C.; Musick, M. D.; Davis, J. A.; Walter, D. G.; Jackson, M. A.; Guthrie, A. P.; Natan, M. J. *J. Am. Chem. Soc.* **1996**, *118*, 1148–1153.
(16) Park, S. H.; Im, J. H.; Im, J. W.; Chun, B. H.; Kim, J. H. *Microchem. J.* **1999**, *63*, 71–91.
(17) Schmitt, J.; Machtle, P.; Eck, D.; Mohwald, H.; Helm, C. A. *Langmuir* **1999**, *15*, 3256–3266.
(18) Kim, T.; Lee, C. H.; Joo, S. W.; Lee, K. *J. Colloid Interface Sci.* **2008**, *318*, 238–243.
(19) Fujiwara, K.; Kasaya, H.; Ogawa, N. *Anal. Sci.* **2009**, *25*, 241–248.
(20) Arcidiacono, S.; Bieri, N. R.; Poulikakos, D.; Grigoropoulos, C. P. *Int. J. Multiphase Flow* **2004**, *30*, 979–994.
(21) Coutts, M. J.; Cortie, M. B.; Ford, M. J.; McDonagh, A. M. *J. Phys. Chem. C* **2009**, *113*, 1325–1328.
(22) Seitz, O.; Chehimi, M. M.; Cabet-Deliry, E.; Truong, S.; Felidj, N.; Perruchot, C.; Greaves, S. J.; Watts, J. F. *Colloids Surf., A* **2003**, *218*, 225–239.
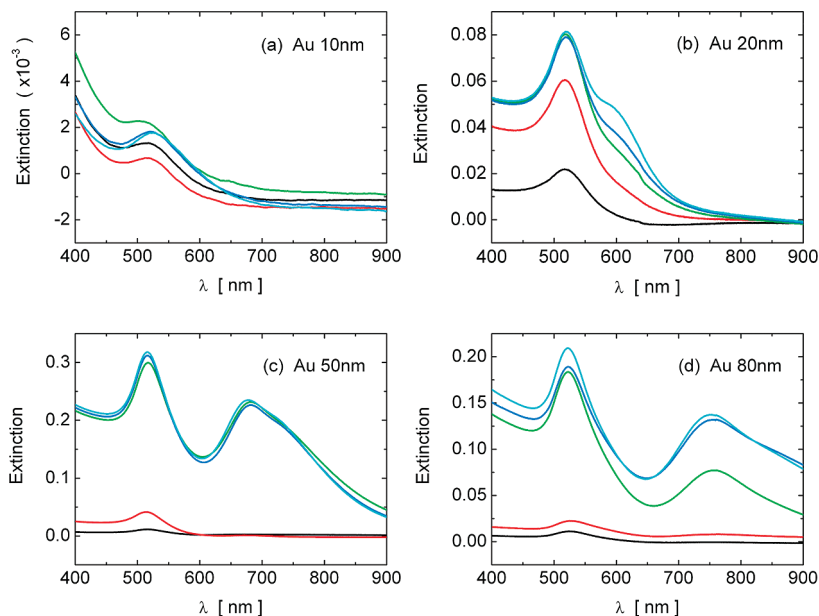
Figure 1. Extinction spectra of APTMS silanized glass substrate, immersed in a solution of gold NPs of (a) 10, (b) 20, (c) 50, and (d) 80 nm in diameter. Black curves correspond to 30 min immersion time, red to 2 h, green to 1 day, blue to 3 days and cyan to 6 days.

this procedure, the glasses were immersed into the gold NP solution kept at room temperature, without any mixing applied. The immersion was done for different amounts of time—30 min, 2 h, 1 day, 3 days, and 6 days—and then washed and dried. This was done for particles of average diameter of 10, 20, 50, and 80 nm in aqueous solution with pH 5, 6, 7, and 7, respectively. Particles size has a coefficient of variation less than 8%, as reported by the seller. All the colloids were surrounded by negatively charged citrates, and there were traces of citrate, tannic acid, and potassium carbonate in the solution, as products of the synthesis. The concentrations of the NPs are 5.7×10^{12}, 7.0×10^{11}, 4.5×10^{10}, and 1.1×10^{10} NPs/mL for the 10, 20, 50, and 80 nm, respectively.

3. Results and Discussion

Extinction spectra and particle counting statistics were recorded for the complete set of samples, i.e., for each NP size and the five different immersion times. Measurement of the extinction (absorption plus scattering) spectra are shown in Figure 1. Collective electronic excitations, or surface plasmons, sustained by the metal NPs can be resonantly excited by the incoming optical field at a given wavelength, producing a sharp increment in both the absorption and scattering cross section of the samples, as can be seen in Figure 1.

For low immersion times, spectra show only one peak which corresponds to the excitation of the plasmon of an isolated NP. As is well-known, new features appear in the spectra when NPs start to form aggregates.[23] This effect can clearly be observed for the samples with longer immersion times. If we consider, for the moment, that the appearance of a new peak comes mainly from the presence of dimers, we can estimate the distance between the two NPs forming the aggregate by comparing our results with the calculations in refs 24–27. Ahead in this work we will address carefully what kind and how many aggregates are present in the samples as a function of time, showing the need to perform particle counting besides the
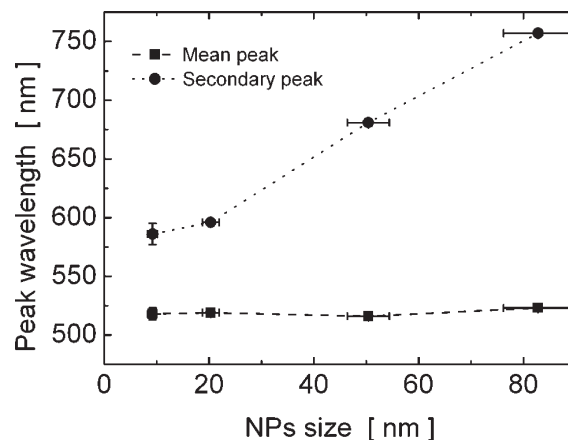

Figure 2. Main and secondary peak wavelengths in the extinction spectra of Figure 1.

optical spectra, but so far, it is a rather good approximation to consider only dimers for having an estimate of the distance.

In Figure 2 we plot the wavelength of the main and secondary peak as a function of NP size, obtained from data shown in Figure 1. Within our spectral resolution, we cannot distinguish differences in the position and width of the secondary peak for samples with different immersion times at a given NP size. The spectral position of the longitudinal plasmon in a NP dimer is strongly dependent on the distance between the NPs, when that distance is lower than about one diameter, border to border.[25,28] It seems from the data that there is not a progressive change in the secondary peak position, suggesting that although the dimer formation is progressive in time, the mean distance between NPs is always at around a fixed mean value. Actually, the cross section of the secondary peak in the extinction spectrum provided by a dimer close to contact is much higher than the contribution from one with a larger distance. From our data, the distance which corresponds to the position of the peak according to many references in the literature[24–27] is about 0.5 nm for all NPs sizes. This distance is on the order of the size of a citrate molecule.

(23) Quinten, M.; Kreibig, U. *Surf. Sci.* **1986**, *172*, 557–577.
(24) Khlebtsov, B.; Melnikov, A.; Zharov, V.; Khlebtsov, N. *Nanotechnology* **2006**, *17*, 1437–1445.
(25) Romero, I.; Aizpurua, J.; Bryant, G. W.; García de Abajo, F. J. *Opt. Express* **2006**, *14*, 9988–9999.
(26) García de Abajo, F. J. *J. Phys. Chem. C* **2008**, *112*, 17983–17987.
(27) Danckwerts, M.; Novotny, L. *Phys. Rev. Lett.* **2007**, *98*, 026104.

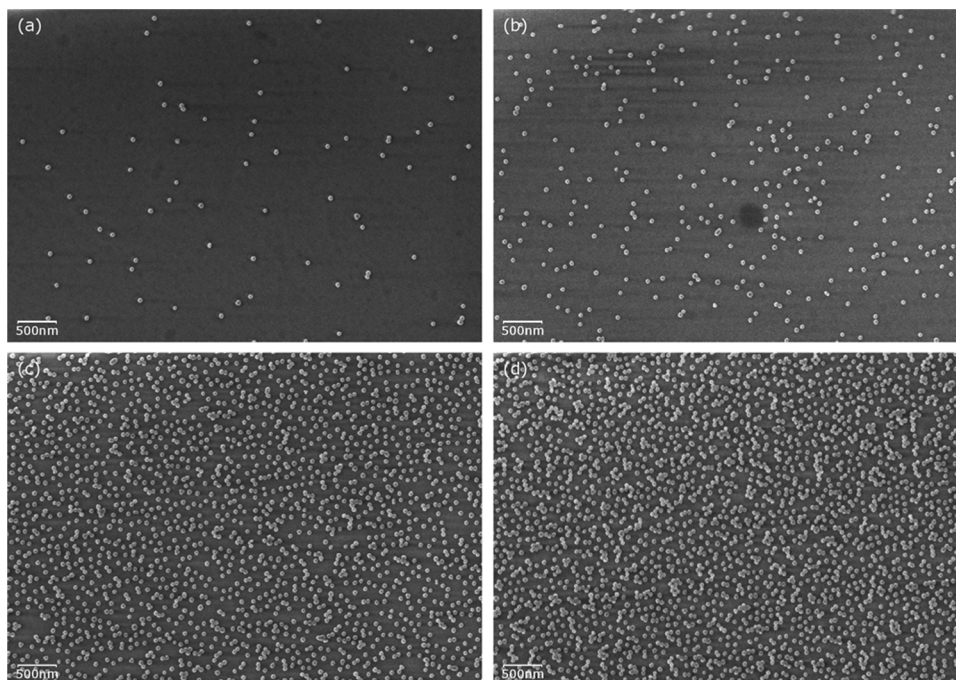(28) Encina, E. R.; Coronado, E. A. *J. Phys. Chem. C* **2010**, *114*, 3918–3923.

Figure 3. Scanning electron microscope (SEM) images of 50 nm gold NPs on silanized glass substrates after immersion times of (a) 30 min, (b) 2 h, (c) 1 day, and (d) 6 days. Pictures clearly show the increment on the coverage with the immersion time and the aggregation of NPs in the last images.

The main peak in the spectra accounts for the dynamics of the NP coverage on the silanized glass. The OH groups adsorbed on the SiO_2 substrate are replaced with the APTMS molecules, which covalently bond to the glass by the Si on the APTMS molecule and the oxygen at the SiO_2 surface. Besides, the APTMS molecules attach each other,[29−31] and as a result, the aminosilane molecules form a very stable and resistant monolayer. Amino groups, weakly protonated, are oriented to the aqueous solution and away from the substrate. Since the solution is slightly acid, protons attach to the amino groups, which become positively charged:

$$NH_2 + H^+ \rightleftharpoons NH_3^+ \tag{1}$$
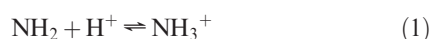
In the early stages, the NPs in solution bump the surface of the glass with APTMS and electrostatically attach to it with high affinity. After a time, the stuck negatively charged NPs and the ions present in the solution which are close to the surface form a boundary layer and screen the positive charge of the APTMS. As a result, the NP coverage saturates when the charges are at equilibrium. This dynamics of coverage is embodied by the behavior of the amplitude of the main peak in Figure 1.

Although the measurement of the spectra is a good beginning to understand the underlying processes, it is not easy to extract from them the number and nature of the interacting particles, since the extinction coefficients are related with the cross section of a variety of unknown objects. Therefore, we complement this measurement with the NP counting statistics taken from the SEM images of the samples.

Typical SEM images are shown in Figure 3. The counting statistics was performed over about 8000−40000 NPs, depending of the NP size.

3.1. Coverage Dynamics. Making the assumption that the surface of the substrate is uniform, the spherical NPs with diameter d are adsorbed to the substrate with a probability p (between 0 and 1). If we call n the number of NPs attached to the substrate per unit of area at a given time t and A the number of collisions NP−substrate per unit of time and area, then we have

$$dn(t) = \frac{n_{sat} - n(t)}{n_{sat}} pA dt \tag{2}$$

where n_{sat} is the saturation number of NPs, produced by the electrostatic repulsion. The maximum number of NPs in a hexagonal close-packed geometry, covering a unit area, n_{max}, is

$$n_{max} = \frac{2}{\sqrt{3}d^2} \tag{3}$$

If we consider an effective diameter of the NPs, $d + s$, then

$$n_{sat} = \frac{2}{\sqrt{3}(d+s)^2} = \frac{d^2}{(d+s)^2} n_{max} \tag{4}$$

where s is related with the average length range of the electrostatic repulsion. If we define the coverage as $c(t) = n(t)/n_{max}$ and the saturation coverage as $c_{sat} = n_{sat}/n_{max} = d^2/(d+s)^2$, hence, from eq 2 we obtain

$$\frac{dc}{c_{sat} - c} = \frac{dt}{\tau_c} \tag{5}$$

where $\tau_c = n_{sat}/(pA)$ is a characteristic time for the coverage process. By integrating eq 5, the time behavior of the coverage results:

$$c(t) = c_{sat}(1 - e^{-t/\tau_c}) \tag{6}$$

The coverage should be proportional to the amplitude of the main peak in spectra of Figure 1, plotted in Figure 4a. We show the amplitude of the main peak from the extinction curve, as a function of the immersion time, for each NP size studied. Note that the general behavior is similar for all the NP sizes: the amplitude
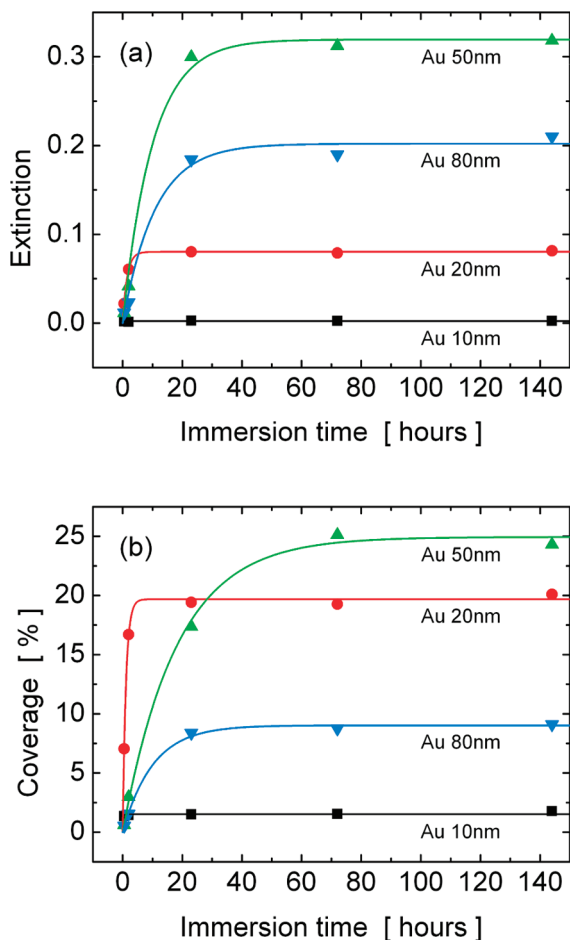
(29) Chauhan, A. K.; Aswal, D. K.; Koiry, S. P.; Gupta, S. K.; Yakhmi, J. V.; Sürgers, C.; Guerin, D.; Lenfant, S.; Vuillaume, D. *Appl. Phys. A: Mater. Sci. Process.* **2008**, *90*, 581–589.

(30) Waddell, T. G.; Leyden, D. E.; De Bello, M. T. *J. Am. Chem. Soc.* **1981**, *103*, 5303–5307.

(31) Vakarelski, I. U.; Brown, S. C.; Moudgil, B. M.; Higashitani, K. *Adv. Powder Technol.* **2007**, *18*, 605–614.

Figure 4. Evolution of (a) the intensity of the main peak of the extinction spectra of Figure 1 and (b) coverage obtained by NPs counting statistics as a function of the immersion time of glass substrates in gold colloids. Lines correspond to fitting with eqs 6 and 14 in the text.

Figure 5. (a) Characteristic coverage time, τ_c, taken from the spectra and NP counting statistics. (b) Extinction to coverage ratio at long times as a function of the NPs diameter. The linear dependence shows the equivalence of the two independent experiments.

grows and then reaches a plateau. Fitting the curves with eq 6, the characteristic coverage time, τ_c, can be obtained for each NP size. The time constants are 16 min, 1.5 h, 10 h, and 11 h for NPs diameter of 10, 20, 50, and 80 nm, respectively.

Figure 4b shows the analysis of the NP counting data obtained from the SEM images. We plot the total number of NPs as a function of the immersion time. The total number of NPs is represented by the coverage, c, where 100% corresponds to a hexagonal close packing of spheres (eq 6). As a first insight we observe that the time constants and shape of these curves are coincident with the behavior of the main spectral peaks, shown in Figure 4a.

For 20 and 50 nm NPs, the maximum coverage reached is dictated by the geometrical and electrostatic effects. The probability to bump into a free space on the substrate is very low if the distance between the NPs is already on the order of one diameter. Note, for example, that 25% of coverage corresponds to a mean distance of exactly one diameter in a hexagonal arrange. On the other side, for 10 and 80 nm NPs, the coverage reached is much lower, suggesting that the saturation is purely electrostatic. In these cases the NP surface negative charge is higher, and then, the equilibrium with the total APTMS positive charge is reached with a lower number of NPs. For testing this argument, we immersed a sample with 10 nm NPs already attached to a substrate into the solution with the 50 nm NPs, and almost no one 50 nm NP stuck to the substrate.

As a summary, Figure 5a shows the values of τ_c obtained from both methods. The figure shows that, independently of the
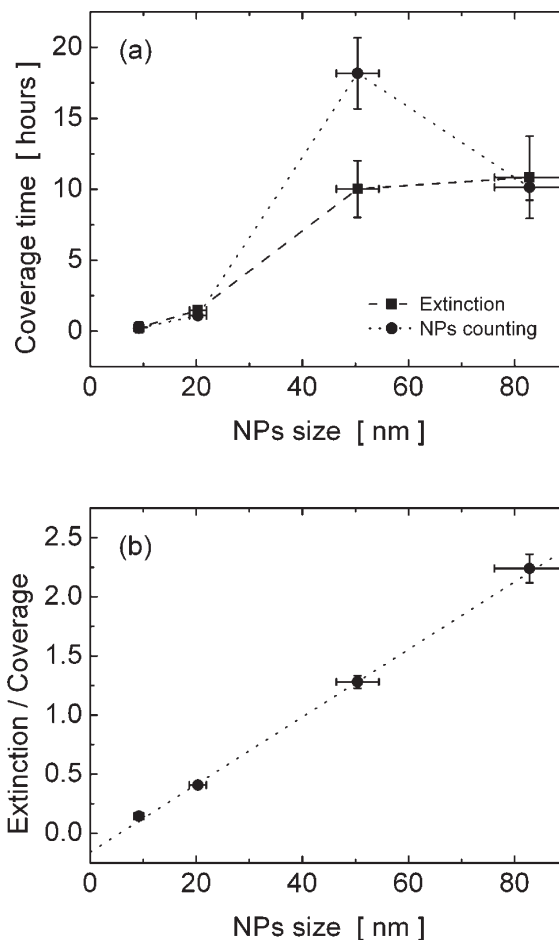
coverage saturation values, τ_c increases with the size of the NP. The coincidence between both methods is evident, despite some deviation for results from the 50 nm NPs. This may have been due to rather low counting statistics over those samples.

At this point we check the equivalence between the two independent experiments done so far, i.e., the measurement of the extinction spectra and the NP counting on the SEM images. If we call E_{sat} the amplitude of the main peak of the extinction curve at long times, we write the ratio between the extinction and counting data as

$$\frac{E_{sat}}{c_{sat}} = \frac{C_{ext} 2 n_{sat}}{n_{sat}/n_{max}} = 2 C_{ext} n_{max} \quad (7)$$

where C_{ext} is the extinction coefficient and 2 is added since the extinction is taken on a glass substrate with NPs deposited on both sides. As C_{ext} is proportional to the volume, d^3, and n_{max} to $1/d^2$, therefore, eq 7 should be linear with d. This behavior is shown in Figure 5b, which allows us to gain confidence on both experiments. Moreover, as the extinction coefficient is $C_{ext} = C_0 d^3$, a linear fit in Figure 5b gives $C_0 = 12.4 \pm 1.8 \ \mu m^{-1}$, in excellent agreement with calculations from ref 6, $C_0 = 14.0 \pm 0.9 \ \mu m^{-1}$.

Using the values of τ_c, we also can estimate some average velocity of the NPs in solution. In effect, if we define n_{sol} as the number of particles in solution per unit volume (i.e., NP concentration), then pA/n_{sol} is that velocity and can be calculated from

$$pA = \frac{c_{sat} n_{max}}{\tau_c} = \frac{E_{sat}}{C_{ext} \tau_c} \quad (8)$$
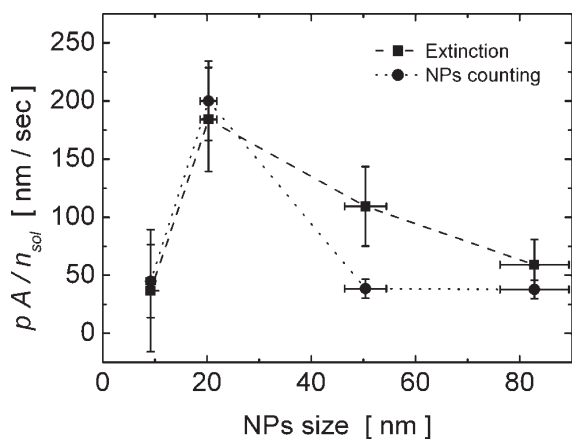
Figure 6. Effective collision speed of NPs from the colloidal solution to the glass surface, taken from the spectra and NP counting statistics, using eq 8.
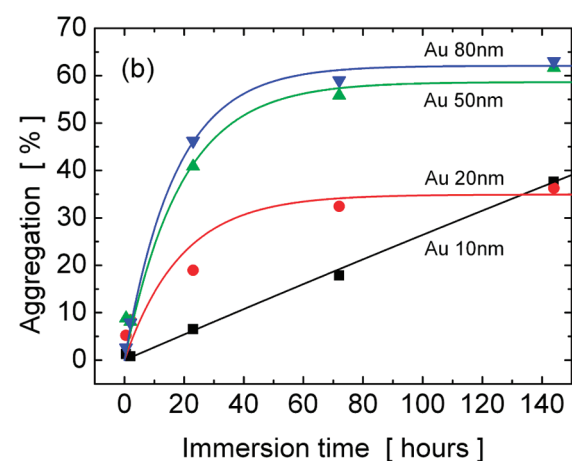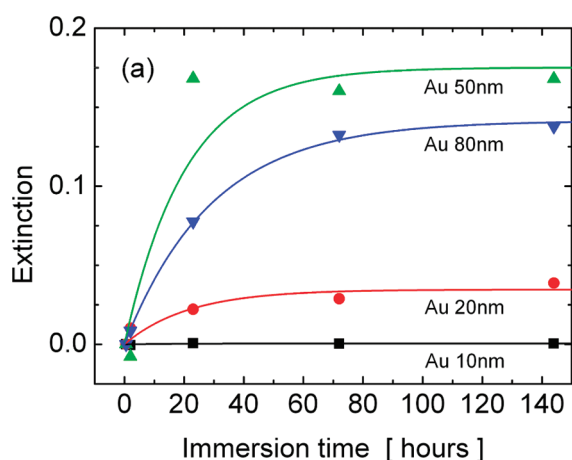

Figure 7. Evolution of (a) the intensity of the secondary peak of the extinction spectra of Figure 1 and (b) aggregation obtained by NPs counting statistics as a function of the immersion time. Lines correspond to fitting with eqs 6 and 14 in the text.

where the second and third terms in eq 8 are the experimental values taken from the fit of the extinction and counting data, respectively, and C_{ext} is given by the slope of Figure 5b. Figure 6 shows pA/n_{sol} for the different NP sizes. The maximum value is about 200 nm/s, reached by the 20 nm NPs, and decreases for bigger NPs, as it is expected due to energy transfer by molecules in a Brownian motion.
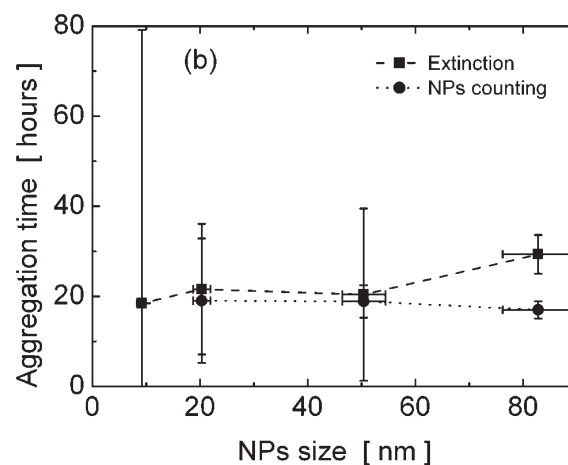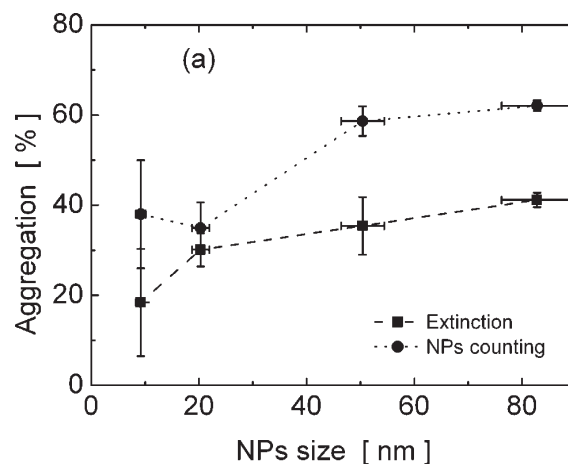

Figure 8. (a) Final fraction of aggregated NPs as a function of the NPs size, obtained by the asymptotic values of the functions fitted in Figure 7. (b) Characteristic aggregation time on the same data.

For the smallest NPs, the adsorption is reduced because of the higher electric charge, as discussed before.

3.2. Aggregation Dynamics. NPs attached electrostatically to the amino groups have mobility and can migrate randomly over the APTMS molecules. Initially, the electrostatic repulsion between NPs keeps them away, ending up in a homogeneous and almost equispaced distribution on the surface. However, the hydrophobic nature of gold tends to aggregate the NPs. The occasional collisions between NPs which are continuously moving induce the formation of small aggregates at the beginning and higher order aggregates at a further time. This process is the so-called sintering, characterized for the reduction of the exposed surface in order to minimize the Gibbs free energy. At the same time that the clusters are formed, empty spaces left on the surface could, in principle, be filled by new NPs. However, the total mean charge near the surface does not change, and as a consequence, the arrival of new NP is not allowed due to the electrostatic repulsion.

Because of the hydrophobic nature of gold, citrate molecules tend to surround them in the aqueous solution of NPs. Once they reach the substrate, the NPs are adsorbed to the glass in two different ways. Some of them are pinned by a van der Waals bond directly to the amino group of the APTMS (NH_2), while others attach electrostatically to the protonated amino (NH_3^+, see eq 1) through the negative charge of the citrates. We assume that the first group has a much higher mobility over the APTMS than the second one, and as a result, only a fraction of the total number of NPs, say n_m, can migrate.
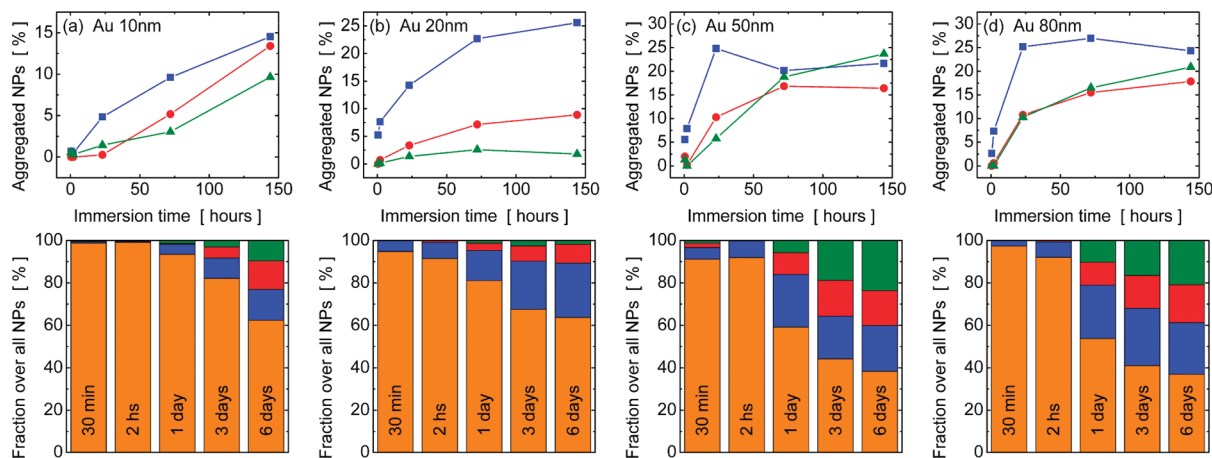
Figure 9. Fraction of isolated NPs (orange), dimers (blue), trimers (red), and clusters of more than three NPs (green) obtained by counting statistics as a function of immersion time in (a) 10, (b) 20, (c) 50, and (d) 80 nm gold colloids.

If we consider that the NPs which can migrate have a probability p' to be aggregated after finding another NP or cluster of NPs, then the increment dn_a of the number of aggregated NPs, n_a, is

$$dn_a(t) = (2A_{iso-iso}(t) + A_{iso-cl}(t))p' \, dt \qquad (9)$$

where $A_{iso-iso}$ is the number of collisions, per unit of time and area, between two isolated NPs traveling over the surface and A_{iso-cl} between an isolated NP and a cluster, being

$$A_{iso-iso} = k(d)\frac{(n_m - n_a)^2}{2}, \quad A_{iso-cl} = k(d)(n_m - n_a)n_a \quad (10)$$

where $k(d)$ depends on the 2D velocity of the NPs and the cross section of the NPs, which are parameters dependent on the size, d. By replacing eqs 10 in eq 9, we obtain

$$dn_a = (n_m - n_a)n_m p' k(d) \, dt \qquad (11)$$

If we define $\theta = n_a/n$ as the fraction of the aggregated NPs at a given time t, then $dn_a = n \, d\theta + \theta \, dn \approx n \, d\theta$. Hence, eq 9 becomes

$$\frac{d\theta}{\theta_{sat} - \theta} = (1 - e^{-t/\tau_c})\frac{dt}{\tau_a} \qquad (12)$$

where $\theta_{sat} = n_m/n$ is the maximum fraction of aggregated NPs which can be reached and $\tau_a = 1/(\theta_{sat}c_{sat}p'k(d))$ is an aggregation characteristic time. Finally, the temporal dependence of θ is

$$\theta(t) = \theta_{sat}\left(1 - \exp\left[-\frac{1}{\tau_a}(t - \tau_c(1 - e^{-t/\tau_c}))\right]\right) \qquad (13)$$

This model could be extended and refined by adding other contributions to the collisions considered in eq 9, e.g., the aggregation due to collisions with the fixed NPs, clusters with clusters, clusters with different sizes, etc. Any additional contribution would add more complexity to eq 13 but cannot be tested with the present experiment. What is important here is that the aggregation follows an exponential-like function with a characteristic time and a saturation value. Moreover, since τ_a is considerably greater than τ_c, eq 13 can be approximated by

$$\theta(t) = \theta_{sat}(1 - e^{-t/\tau_a}) \qquad (14)$$

Figure 7 shows the analysis of the aggregation process. In Figure 7a the amplitude of the secondary peak from the extinction spectra of Figure 1 is shown. Figure 7b plots the interacting NPs taken from the SEM images, where the percentage of interacting NPs is calculated over the total number of NPs, n.

Using eq 14, we fit the spectra and particle counting data, obtaining very good results, as can be seen in Figure 7. In Figure 8 the obtained values for the relevant parameters of the experiment are plotted. It is shown in the figure that the final fraction of aggregated NPs grows with the NP size and that the aggregation characteristic time is on the order of 20−30 h.

Finally, Figure 9 shows the number of dimers, trimers, and higher order aggregates as a function of immersion time and the histograms weighting against the number of isolated NPs, dimers, trimers, and higher order aggregates. We see that at short times only dimers appear, while the number of trimers and higher order aggregates start to increase only after 1 day. This fact reinforces the idea that only the isolated NPs have an appreciable mobility.

4. Conclusions

In this work we studied the dynamics of coverage and aggregation of gold NPs over silanized glass substrates. Two complementary experiments—measurement of the extinction and particle counting statistics—are shown to be equivalent describing the coverage process. For the aggregation, the counting of particles is necessary to clearly separate the dynamics of formation of dimers, trimers, and higher order aggregates. It is shown that both coverage and aggregation processes are described by two main parameters: a characteristic time and a saturation value. The dependence of those parameters with physicochemical quantities is included in a model that describes accurately the measured data. We would like to emphasize that the development of a model, and the very good accordance with the experimental data, turns this work into an excellent predictive tool to prepare NP samples when a given coverage and aggregate percentage are desired.